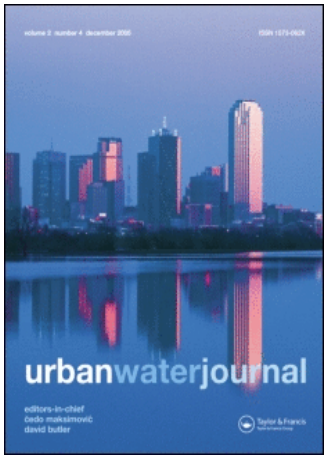

Urban Water Journal
Publication details, including instructions for authors and subscription information:
http://www.informaworld.com/smpp/title~content=t713734575

Scaling the solute transport characteristics of a surcharged manhole

S. Lau [a]; V. Stovin [a]; I. Guymer [b]
[a] Department of Civil and Structural Engineering, The University of Sheffield, Sheffield, UK
[b] School of Engineering, University of Warwick, Coventry, UK

Online Publication Date: 01 March 2008
To cite this Article: Lau, S., Stovin, V. and Guymer, I. (2008) 'Scaling the solute transport characteristics of a surcharged manhole', Urban Water Journal, 5:1, 33 - 42
To link to this article: DOI: 10.1080/15730620701737249
URL: http://dx.doi.org/10.1080/15730620701737249

Urban Water Journal
Vol. 5, No. 1, March 2008, 31–40

Scaling the solute transport characteristics of a surcharged manhole

S. Lau[a], V. Stovin[a]* and I. Guymer[b]

[a]*Department of Civil and Structural Engineering, The University of Sheffield, Mappin Street, Sheffield S1 4DT, UK;*
[b]*School of Engineering, University of Warwick, Coventry CV4 7AL, UK*

Guymer *et al.* (2005) presented the results of experimental work that explored the effects of diameter and surcharge on the solute transport processes occurring in surcharged manholes. A threshold surcharge level was identified, with two contrasting hydraulic regimes being observed at surcharge depths above and below the threshold value. In this study, a 1:3.67 physical scale model of an 800 mm diameter manhole has been built to investigate the effects of scale on hydraulic and solute transport characteristics. Dye tracing experiments and energy loss measurements have been made in the physical scale model. The results suggest that geometric scaling laws may be used to characterise the flow regime, and to identify the threshold surcharge depth. Solute transport characteristics are presented in the form of a cumulative residence time distribution (CRTD), in which the *x*-axis (time dimension) is normalised by the nominal residence time (volume/discharge). The CRTDs reveal the effect of hydraulic regime on solute transport processes, with two distinct characteristic curve shapes corresponding to the two contrasting hydraulic regimes. A preliminary comparison of the normalised CRTD curves for the model and prototype systems suggests that the scale-independent solute transport characteristics of the structure may be characterised by just two dimensionless CRTDs; one for pre-threshold and the second for post-threshold hydraulic conditions.

Keywords: dispersion; energy loss; hydraulic regime; manhole; cumulative residence time distribution (CRTD); sewer, solute transport; surcharge

1. Introduction

Solute transport processes affect the performance of a wide range of water engineering structures. In the context of urban drainage, future legislation (certainly in Europe) is likely to focus increasingly on the effects of dissolved pollutants. The effects of dispersion may act to reduce or eliminate first foul flush effects or to moderate peak concentrations associated with intermittent discharges. Dispersion also implies that pollutant materials may be present a long time before and after predictions based on mean travel time would suggest. Urban drainage network models that predict the transport of dissolved substances are increasingly used. Some of the models transport the pollutants by advection only, while others also account for the effects of dispersion. At present there is limited knowledge regarding appropriate values for the model parameters. In some instances laboratory measurements have been conducted (see e.g. Guymer *et al.* 2005), but the applicability of laboratory-scale derived parameters to full-scale structures in the urban drainage system, i.e. scalability of these parameters, is not clearly understood.

Guymer *et al.* (2005) presented comprehensive data from laboratory experiments on the travel times and dispersion associated with a solute pulse passing through a surcharged manhole. Of particular interest in this work was the identification of a threshold surcharge level at which the solute transport characteristics indicated a sharp transition between pre- and post-threshold levels. At surcharge levels below the threshold, the travel times increased linearly with surcharge, while above the threshold travel times dropped to a low and constant value. Laboratory visualisation techniques revealed two distinct hydraulic regimes in the manhole; pre-threshold the flow field was dominated by a chaotic and swirling motion throughout the manhole volume that promoted full mixing. Post-threshold the flow field comprised two separated flow regimes – a dead zone was formed in the upper volume of fluid, while the majority of the incoming flow passed straight through the manhole, short-circuiting the upper storage volume. A computational fluid dynamics-based study has provided further insights into the flow mechanisms that governed these mixing characteristics (Lau *et al.* 2007).

*Corresponding author. Email: v.stovin@sheffield.ac.uk

ISSN 1573-062X print/ISSN 1744-9006 online

DOI: 10.1080/15730620701737249
http://www.informaworld.com

The present study aims to investigate how scaling affects both the hydraulic and solute transport characteristics of surcharged manholes. A 1:3.67 physical scale model of the 800 mm diameter manhole (prototype) has been constructed, and solute transport experiments have been undertaken to evaluate the travel time and dispersion characteristics. The present work also quantifies the effects of discharge and surcharge on energy loss for this particular manhole configuration (ratio of manhole diameter to pipe diameter), which has not been considered in previous manhole studies (O'Brien 1999, Dennis 2000, Guymer *et al*. 2005).

2. Experimental facilities and procedure

The self-contained recirculating system used for this study is similar to the one described in Guymer and O'Brien (2000). It comprised a constant header tank and a storage sump from which a submersible pump continuously circulated water through the system. The system had a maximum discharge capacity of 16 l/s and the flow rate through the test section (Figure 1) was controlled by a discharge control valve 4 m upstream of the manhole. The test section consisted of a horizontal Perspex pipe 24 mm internal diameter (ID) and a 218 mm ID manhole. The discharge through the manhole apparatus was monitored using a Venturi meter installed 1.24 m downstream of the manhole outlet. This measurement device was connected to two 25 mm diameter manometers with measurement scales attached. The flow rate measurement system was calibrated *in situ* using a volumetric method and could quantify a range of flow rates from 0.1 to 2 l/s with an accuracy to 0.01 l/s. A surcharge control tank was positioned at the downstream end of the system. The tank inlet was positioned at a lower elevation than the manhole exit. This was to provide sufficient head between the water levels in the manhole and in the surcharge tank such that a complete range of surcharges within the manhole could be studied. The water level in the manhole was controlled by modifying the weir height in the tank. Temporal variations in the free water surface within the manhole were recorded using a model H45 water level follower (Armfield). This device could measure water level changes up to 50 mm/s.

Six pressure tappings were installed at 500, 750 and 1000 mm upstream and downstream from the centre of the manhole. The closest downstream tapping point was about 16 pipe diameters downstream of the manhole outlet, at which point it would be expected that a fully turbulent flow profile would have re-established (generally accepted minimum distance is 10 pipe diameters (Howarth 1985)). Each tapping was connected to an 88 mm diameter stilling column with a measurement scale that could be read to an accuracy of 1 mm.

Series 10 fluorometers (Turner Designs) were used to monitor temporal concentration distributions at the sampling stations, which were situated 368 mm upstream and downstream from the manhole centre.

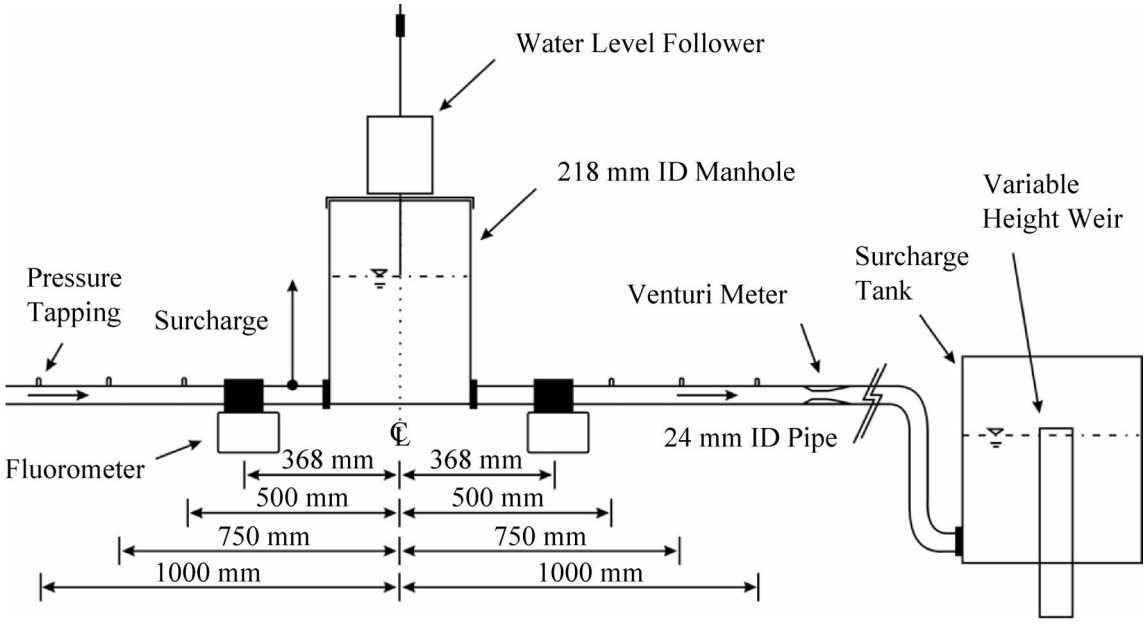

Figure 1. Experimental configuration.

The fluorometers were slightly modified to allow the 30 mm outer diameter (24 mm ID) Perspex pipe to fit the instrument's original configuration for non-intrusive continuous sampling. The pipe cross-sectional concentration was therefore determined without any flow disturbance. In this configuration, the Turner Designs fluorometers are highly susceptible to interference from extraneous light that may intrude into the sampling section. As a result, all pipework and the manhole were fully enclosed with wooden black-out boxes. The two fluorometers were calibrated in-situ following the procedure suggested by O'Brien (1999). Rhodamine WT was used for the dye tracing experiments. The fluorometers were regulated to operate in the linear response region up to dye concentrations 2.5×10^{-7} l/l. In each test run, approximately 25 ml of the dilute solution was introduced in the form of an instantaneous injection into the supply pipe 4 m upstream of the upstream sampling station. This distance, more than 100 pipe diameters, ensured that the solute concentration was cross-sectionally well mixed (approximately Gaussian distribution) at the upstream measurement position.

In the scale model study, five flow rates between 0.25 to 0.5 l/s and ten surcharge depths within the range of 10 and 100 mm have been considered, resulting in five hundred steady flow hydraulic conditions. In each case study, five repeat tracer test runs were performed. In each run, digital readings from the fluorometers and the water level follower were logged simultaneously at 50 Hz for a period of 5 min. The time to peak was generally less than 5 s; in all cases the solute concentration at the downstream measurement position had returned to background levels well within the 5 min cut-off. For the pressure measurement, the manometer readings were recorded three times during each run.

3. Data analysis

Under steady hydraulic conditions, variations in pressure and surcharge level during the experiment were insignificant. Pressure fluctuations shown on the manometers were within ± 1 mm of the mean value. The measurements from the water level follower showed a mean standard deviation during each test of 2 mm over the range of surcharge depths studied, with greater fluctuations being observed at low surcharge depths. In certain circumstances, where the free surface in the manhole fluctuated about a mean depth at high frequency, the water level follower failed to track the surface and gave erroneous readings, for example a signal reading corresponding to a negative surcharge level. These erroneous readings were eliminated before averaging the water level data series.

The energy loss coefficient for the surcharged manhole was estimated from the pressure measurements. The energy loss owing to the manhole, ΔH, is defined as the difference in pressure head at the manhole centreline between the extrapolated upstream and downstream hydraulic lines, obtained from three point measurements (Arao and Kusuda 1999). Values of the coefficient were calculated using the equation below

$$\Delta H = K\frac{u^2}{2g} \tag{1}$$

where u is mean pipe velocity; g is gravitational acceleration; and K is head loss coefficient.

For each individual injection of solute tracer, temporal concentration distributions were recorded from both upstream and downstream fluorometers. The digital data captured from the fluorometers required post-processing to determine the concentration distributions corresponding to the solute. The post-processing procedure comprised calibration, background concentration removal and identification of the start and end points of temporal concentration distributions, i.e. to eliminate noisy background data. The technique for the first two processes is well-established (see e.g. O'Brien 1999, Dennis 2000). However, several techniques have been proposed for the identification of the profile start and end points. Dennis (2000) defined the cut-off as the 10th consecutive data point away from the peak with a concentration value less than 1% of the peak concentration. This technique was tested on the temporal concentration distributions obtained from a straight pipe study. The study employed the same laboratory configuration as Figure 1 but with a 24 mm ID straight pipe replacing the manhole. Results showed that the cut-off technique successfully eliminated the noisy background, whilst keeping the entire solute trace (mass balances of above 99%). This cut-off technique was therefore applied to all manhole tracer profiles. The concentration data were not mass balanced.

4. Results

4.1. Relationship between energy loss coefficient and surcharge ratio

The surcharge ratio is defined as the ratio of surcharge depth (measured with respect to the soffit of the pipe) to manhole diameter, S. The variations of energy loss coefficient with surcharge ratio for the 218 mm diameter manhole are shown in Figure 2. A sharp

transition of the energy loss coefficient between pre- and post-threshold is evident at a surcharge ratio of between 2 and 2.5. At surcharge ratios below the threshold ratio, but above $S = 0.7$, energy loss coefficients appear to increase slightly as a function of surcharge ratio. After the transition, the coefficient values are reduced by half compared with the values in the pre-threshold region, yielding a coefficient value of around 0.45.

At the lowest surcharge ratio considered in Figure 2, there are several data points that fall below the linear trend, with values less than 0.9. This phenomenon is similar to that observed by Arao and Kusuda (1999), shown in Figure 3. In the range of 0 to 0.5 surcharge ratio, their data suggests that energy loss coefficients increased rapidly with surcharge; beyond this region, the rate of increase began to flatten off until the hydraulic transition point, marked by a sudden drop in the energy loss coefficient value, was reached.

The relationship between energy loss coefficient and surcharge ratio observed in the post-threshold region (Figure 2) matches well to the experimental findings of Arao and Kusuda (1999). Immediately after the hydraulic transition, the coefficient values drop significantly to around 0.45 and remain constant thereafter. This value appears to be consistent between the two sets of data, with the exception of the lowest discharge considered in Arao and Kusuda (1999) (0.48 l/s), for which the values of the energy loss coefficient are consistently lower than at other discharges. Arao and Kusuda do not offer an explanation for this. Figure 3 suggests that a secondary peak in energy loss occurred at surcharge ratios of around 3.3 (i.e. three times the surcharge ratio associated with the primary step in energy loss coefficient). As the present laboratory data set does not extend beyond two times the threshold surcharge ratio, it is not possible to comment on the existence or not of a comparable secondary peak. Energy loss coefficient does not appear to be strongly dependent upon discharge, with the exception of the lowest discharge considered in Arao and Kusuda (1999).

The threshold depth for the hydraulic transition differs between the present data set and that presented by Arao and Kusada (1999) (surcharge to pipe diameter ratio of 2.5 compared with 1.0). This reflects the fact that the two studies have considered manholes with different manhole diameter to pipe diameter ratios. Guymer *et al.* (2005) suggested that the threshold depth varies as a linear function of the manhole diameter to pipe diameter ratio, and that the value of the threshold depth can be approximately predicted by reference to jet theory.

4.2. Relationship between travel time and surcharge ratio

Preliminary analysis of the data suggested that neither the advection dispersion equation (ADE)

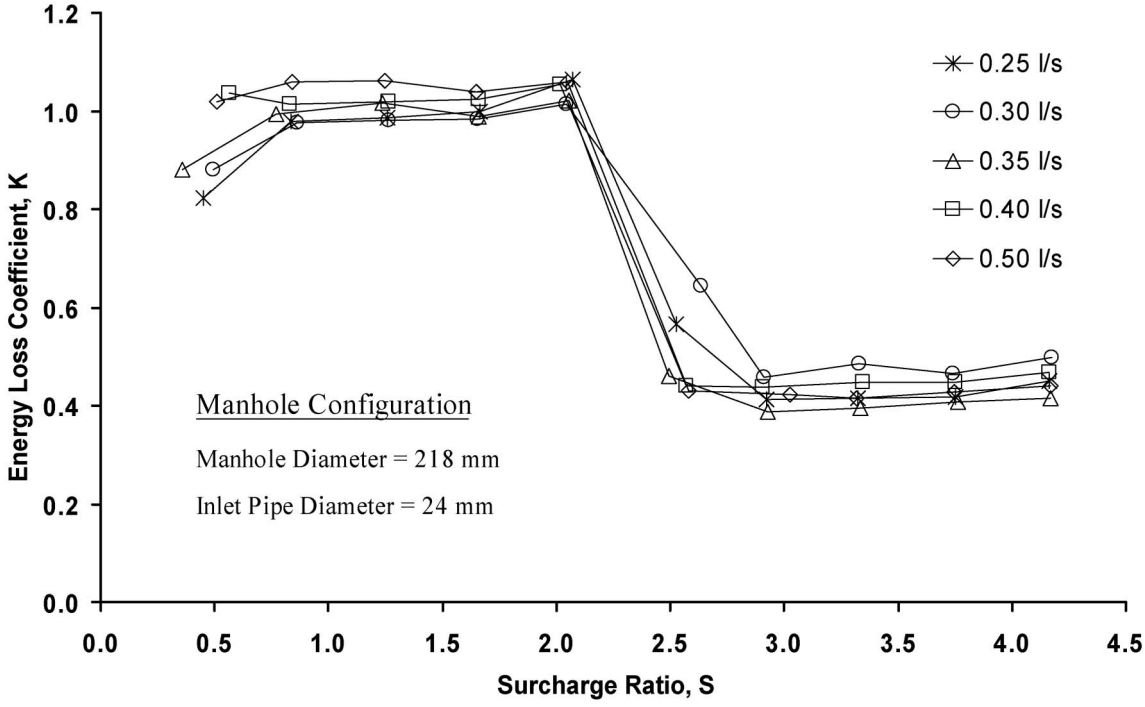

Figure 2. Variations of energy loss coefficient with surcharge ratio for the 218 mm diameter manhole.

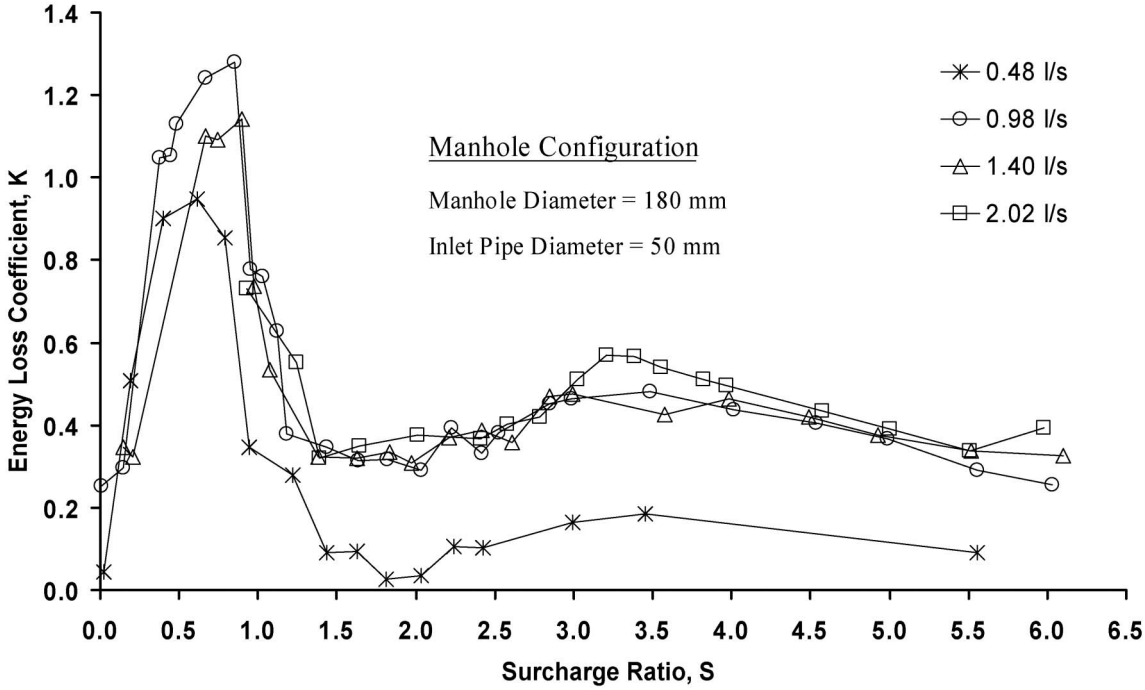

Figure 3. Relationship between energy loss coefficient and surcharge ratio (after Arao and Kusuda 1999).

nor the aggregated dead zone (ADZ) modelling approaches (Guymer *et al*. 2005) provided satisfactory fits to the experimental data (Figure not shown). For example, pre-threshold, predictions made using the two models under-estimated the peak concentration by more than 10% and neither method accurately predicted the recorded shape; post-threshold, the model predictions considerably deviated from the measured profiles at the rising and falling limbs.

In the current paper, the travel time is defined in terms of the cumulative residence time distribution (CRTD). The median travel time (50th percentile), defined as the time difference between the 50th percentile of the upstream and downstream profiles, has been adopted to represent the characteristic travel time of the system.

Values of the median travel time for the scale model are presented in Figure 4. The travel time results are similar to the results presented in Guymer *et al*. (2005) (figure not shown). A sharp transition at a surcharge ratio of between 2 and 2.5 can be clearly identified in the 218 mm diameter manhole data, whereas the threshold surcharge ratio observed in Guymer *et al*. (2005) was approximately 2.5. In the pre-threshold region, travel times vary linearly with surcharge; while post-threshold, travel times drop to a low and nearly constant value. In addition, both sets of results demonstrate an inverse relationship between travel time and discharge.

5. Discussion

5.1. Temporal concentration distributions comparison – prototype and scale manhole

The travel time data for the scale model suggest that the scale model showed similar hydraulic characteristics to the prototype presented in Guymer *et al*. (2005). The threshold depth occurred at a comparable surcharge to pipe diameter ratio, confirming the validity of geometric scaling. Figures 5(a) and 5(b) present comparisons of the downstream distributions in response to an upstream Gaussian temporal concentration distribution. For comparative purposes, the concentrations are normalised with respect to the peak concentration and the downstream temporal concentration distributions are plotted with respect to the first arrival time. The trends in the variations of downstream distribution shape as a function of surcharge are highly comparable in both manhole models. Normalised with respect to the peak, the distributions show no noticeable difference at the rising limbs. The effects of surcharge on the distributions become marked in the shape of the falling limb. In all distributions, the Gaussian-like profile distorts at some point and follows an approximately linear decay.

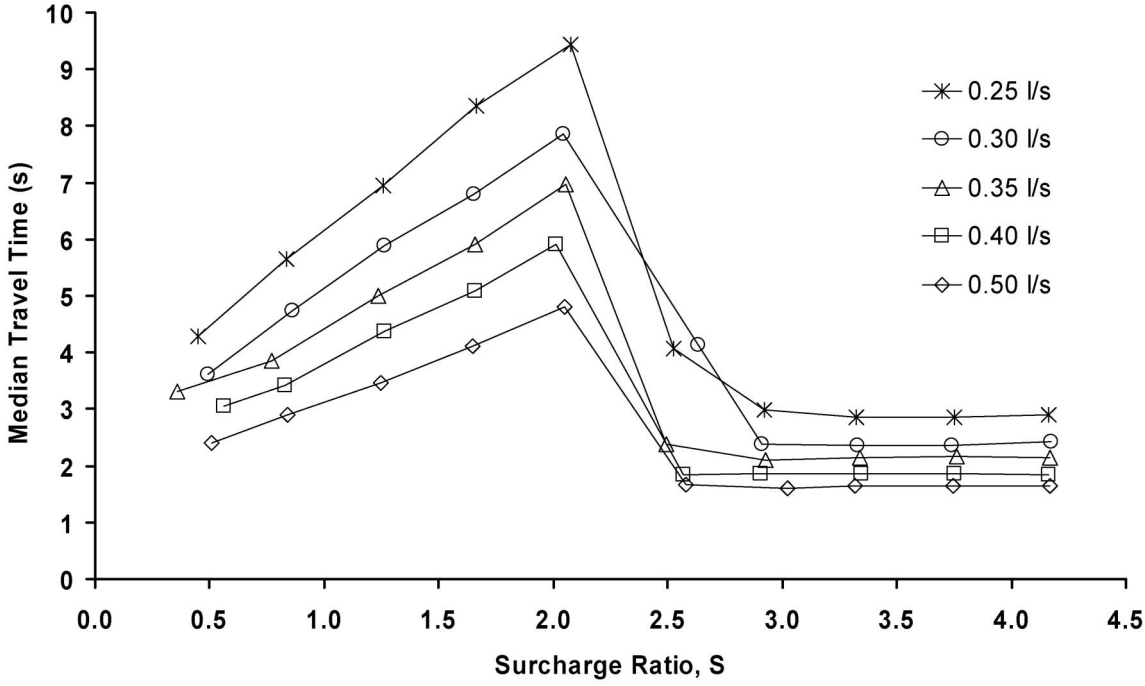

Figure 4. Relationship between median travel time and surcharge ratio for the 218 mm diameter manhole.

5.2. Comparison of cumulative retention time distributions – prototype and scale model

The scalability of the solute transport characteristics is studied via the comparison of CRTDs, shown in Figures 6 and 7 for pre- and post-threshold respectively. The distributions presented in the figures are the cumulative downstream profiles with the y-axis normalised with respect to the total mass of the corresponding upstream distribution and the time axis with nominal travel time, t_n (the total water volume between sampling stations divided by discharge). For presentation purposes, only one surcharge depth is considered for each hydraulic regime; the sample depths have been selected to represent a mid-point from the pre-threshold depth range ($S \approx 1.3$, Figure 6) and a mid-point from the post-threshold dataset ($S \approx 3.3$, Figure 7).

It is evident that, after normalisation, the distributions in each figure tend to collapse onto a single curve, and that no systematic variation arises as a function of discharge. The plots corresponding to different surcharge depths within the same hydraulic regime (not shown) also fall on the same single characteristic curve, implying that the effects of both discharge and surcharge are accounted for in the temporal normalisation process.

Comparison of Figures 6(a) and 6(b) suggests that the basic shape of the pre-threshold CRTD is independent of manhole scale. The near-exponential form of the curve is indicative of instantaneous mixing.

Post-threshold (Figures 7(a) and 7(b)), the downstream distributions reflect a different mixing mechanism. The cumulative concentration distributions appear to consist of two sections, a symmetrical (i.e. Gaussian) profile between mass recovery 0% to about 65% and an approximately linear tail from 65% onwards. The steep slope immediately after the first arrival of the trace indicates that short-circuiting affects 65% of the injected tracer. The rest of the tracer, which has been trapped in the manhole, is released at a relatively slow rate. For example, to achieve 90% of mass recovery, it could take more than four times the normalised median travel time. Note that complete mass recovery was not attained in most of the CRTDs. Loss of mass could result from the cut-off scheme applied to the profiles and, more probably, the instrument noise of the fluorometers at low concentrations. As in the pre-threshold hydraulic regime, comparison of Figures 7(a) and 7(b) suggests that the basic shape of the normalised CRTD is scale-independent.

The analysis presented above suggests that the solute transport characteristics of the surcharged manhole can be summarised in terms of just two CRTDs, one for each of the two identified hydraulic regimes. However, more careful examination of

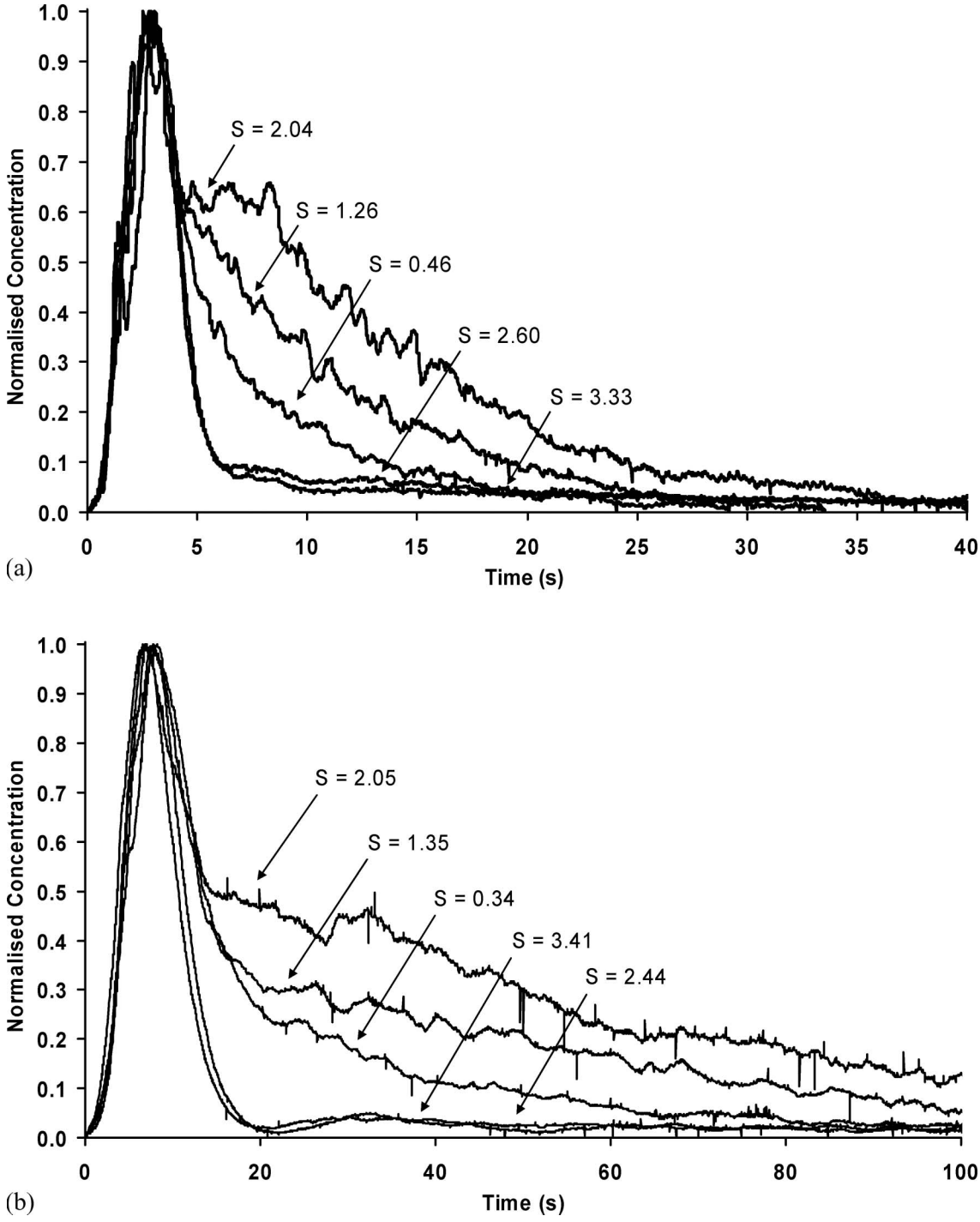

Figure 5. Effects of variations in surcharge on downstream temporal concentration distributions: (a) the scale model operated at 0.3 l/s; (b) the prototype operated at 2 l/s (after Guymer *et al.* 2005).

Figures 6(a) and 6(b) and 7(a) and 7(b) suggests that the curves derived from the two different experimental scale models do not exactly coincide (Figure 8). This is likely to reflect the fact that the characteristics of the upstream distribution (i.e. its shape and duration) differed between the two experimental data sets, and work is underway to generate CRTDs that correspond to instantaneous upstream profiles. Any discrepancies that remain will then need to be accounted for as scale effects for the manhole system.

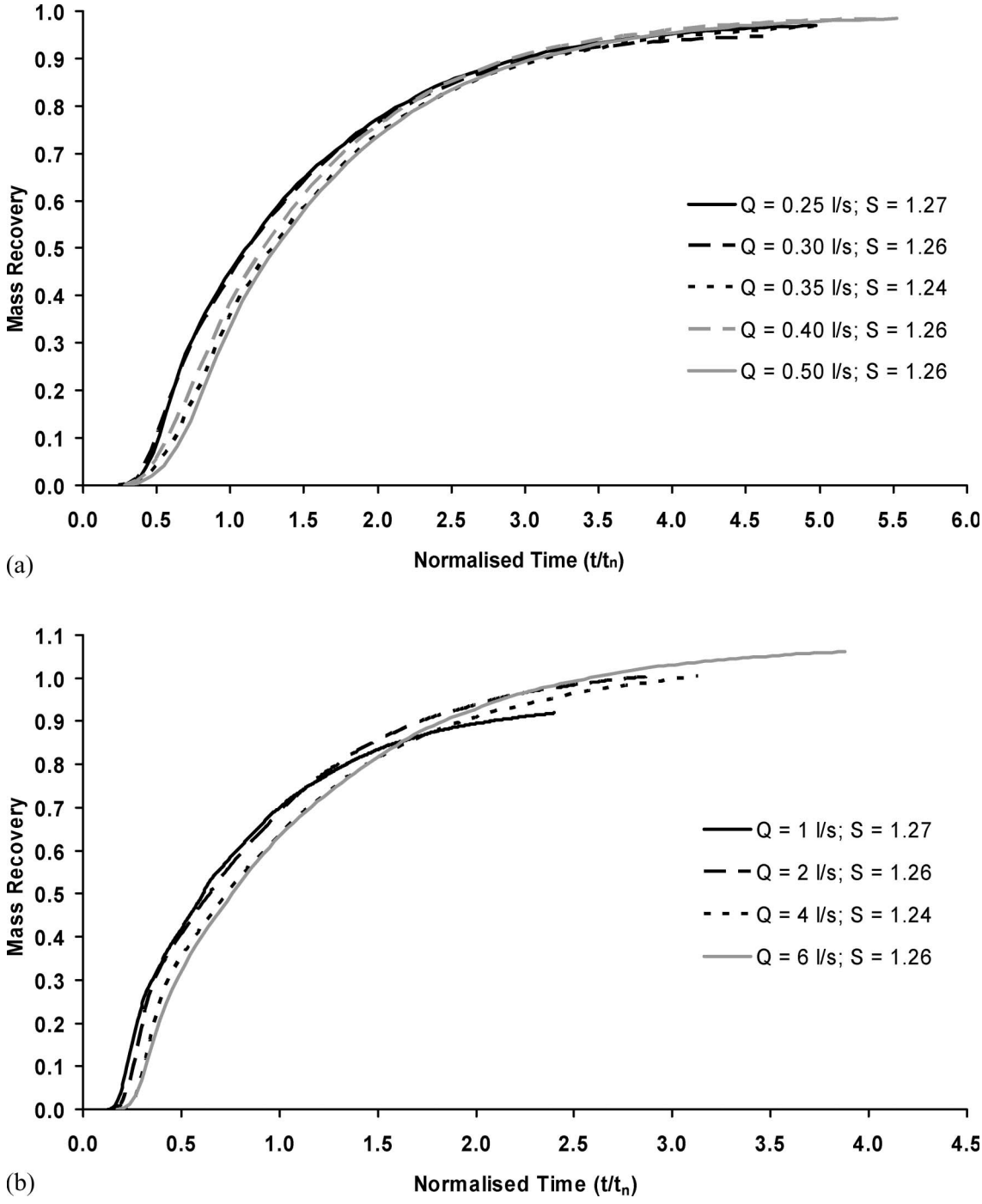

Figure 6. Comparison of pre-threshold cumulative retention time distributions for the manholes: (a) the scale model; (b) the prototype.

6. Conclusions

A 1:3.67 physical scale model of an 800 mm diameter manhole has been constructed and experiments have been undertaken to examine its hydraulic and solute transport characteristics. The energy loss coefficient and the median travel time for the 218 mm manhole show a sharp transition between pre- and post-threshold surcharge depth, and the transition appears at a surcharge ratio of between 2 and 2.5. This ratio matches that observed in an 800 mm manhole, confirming that geometric scaling on the threshold depth is valid.

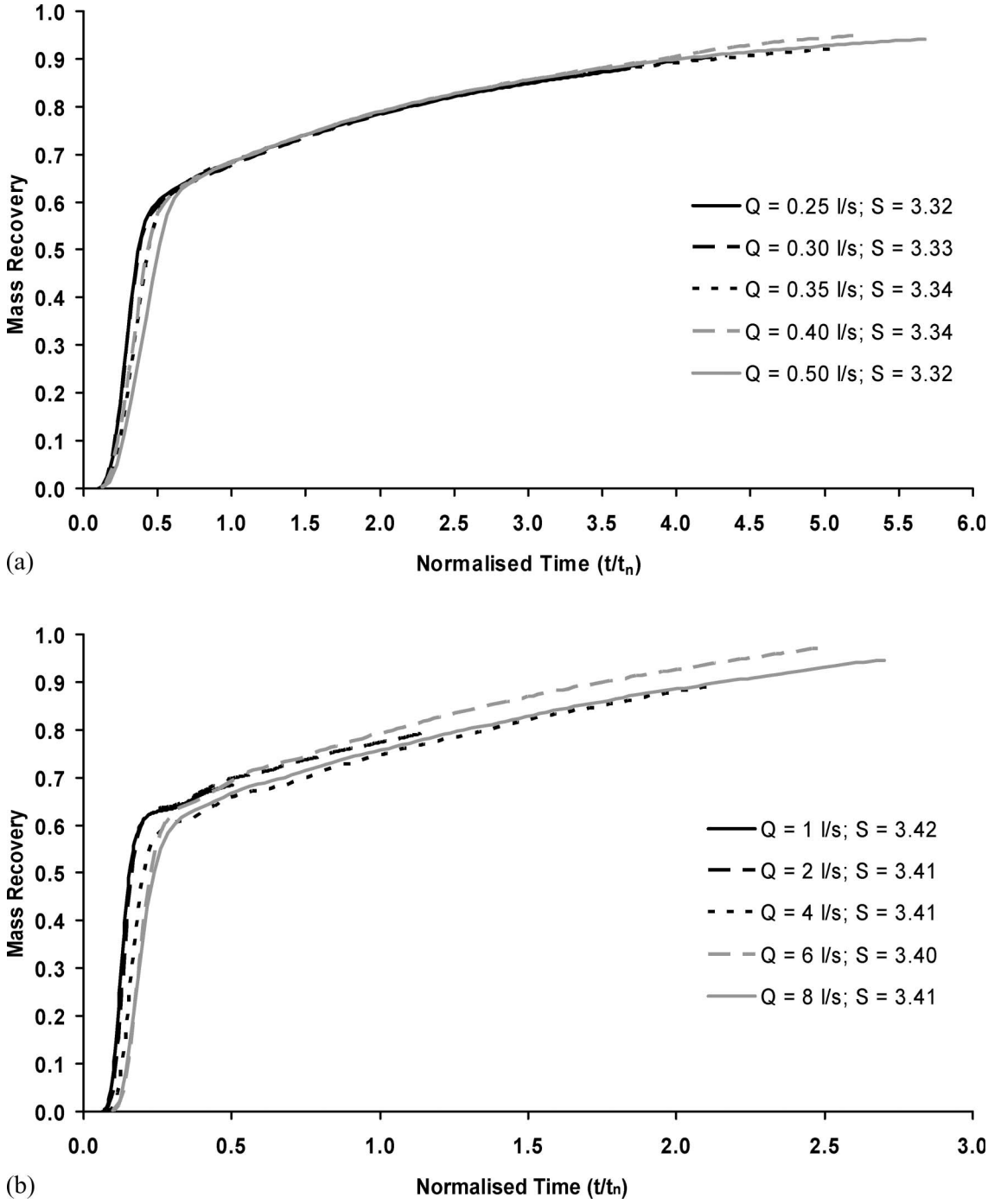

Figure 7. Comparison of post-threshold cumulative retention time distributions for the manholes: (a) the scale model; (b) the prototype.

Scale effects on solute travel time and dispersion characteristics have been considered via the comparison of CRTDs. The normalised CRTDs for each manhole collapse onto a single curve for each of the two hydraulic regimes. The normalised CRTDs of the two differently-sized manhole models also appear to be similar in terms of profile shape, which suggests that the two CRTDs could provide a scale-independent method of characterising the travel time and dispersion characteristics for this type of system.

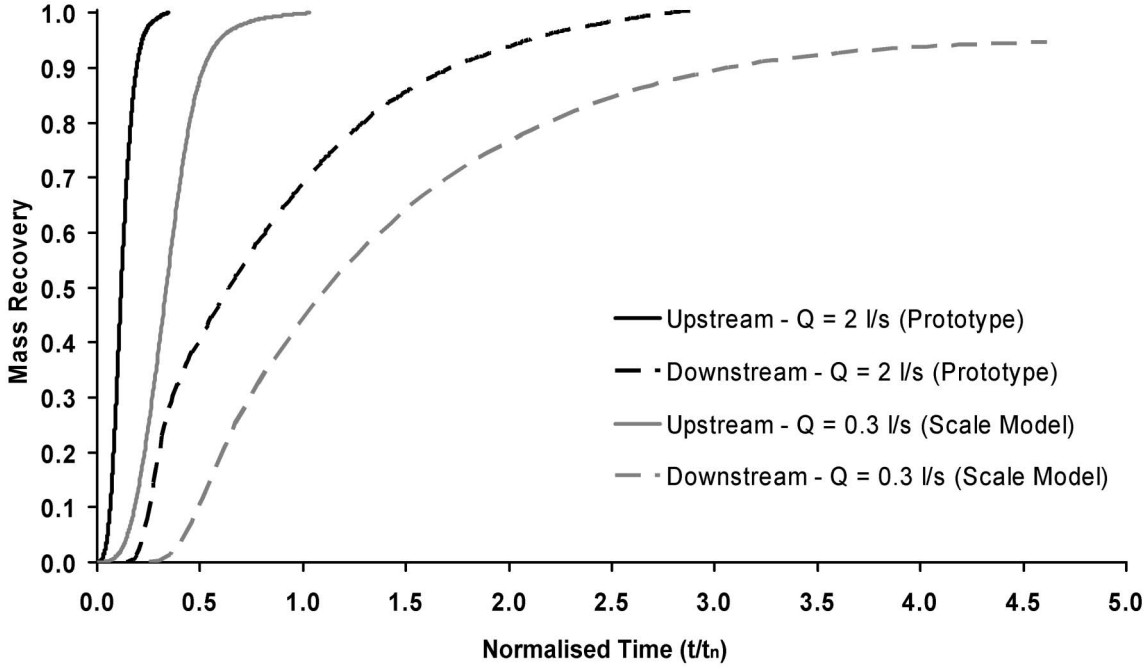

Figure 8. Comparison of pre-threshold upstream and downstream CRTDs at $S = 1.25$ for the two manhole models.

Further work is required to eliminate the influence of upstream concentration profiles in order to verify this hypothesis.

References

Arao, S. and Kusuda, T., 1999. Effects of pipe bending angle on energy losses at two-way circular drop manholes. *In*: *8th International Conference On Urban Storm Drainage*, 30 August–3 September, Sydney. Australia, 2163–2168.

Dennis, P.M., 2000. *Longitudinal dispersion due to surcharged manholes*. Thesis (PhD), The University of Sheffield.

Guymer, I. and O'Brien, R.T., 2000. Longitudinal dispersion due to surcharged manhole. *Journal of hydraulic engineering*, 126 (2), 137–149.

Guymer, I., Dennis, P.M., O'Brien, R.T., and Saiyudthong, C., 2005. Diameter and surcharge effects on solute transport across surcharged manholes. *Journal of hydraulic engineering*, 131 (4), 312–321.

Howarth, D.A., 1985. *The hydraulic performance of scale model storm sewer junctions*. Thesis (PhD), The University of Manchester.

Lau, S.D., Stovin, V., and Guymer, I., 2007. The prediction of solute transport in surcharged manholes using CFD. *Water science and technology*, 55 (4), 57–64.

O'Brien, R.T., 1999. *Dispersion due to surcharged manholes*. Thesis (PhD), The University of Sheffield.